

## III-nitride ultraviolet light-emitting diodes with delta doping

K. H. Kim, J. Li, S. X. Jin, J. Y. Lin, and H. X. Jiang

Citation: *Applied Physics Letters* **83**, 566 (2003); doi: 10.1063/1.1593212

View online: <http://dx.doi.org/10.1063/1.1593212>

View Table of Contents: <http://scitation.aip.org/content/aip/journal/apl/83/3?ver=pdfcov>

Published by the [AIP Publishing](#)

---

### Articles you may be interested in

[Mask-free photolithographic exposure using a matrix-addressable micropixelated AlInGaN ultraviolet light-emitting diode](#)

*Appl. Phys. Lett.* **86**, 221105 (2005); 10.1063/1.1942636

[Polarization of III-nitride blue and ultraviolet light-emitting diodes](#)

*Appl. Phys. Lett.* **86**, 091107 (2005); 10.1063/1.1875751

[Time-resolved electroluminescence studies of III-nitride ultraviolet photonic-crystal light-emitting diodes](#)

*Appl. Phys. Lett.* **85**, 2104 (2004); 10.1063/1.1786372

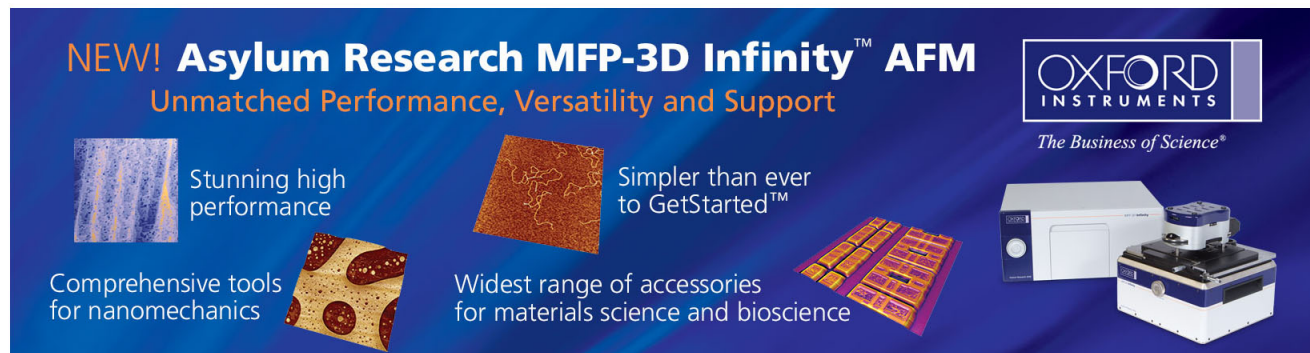
[Enhanced light extraction in III-nitride ultraviolet photonic crystal light-emitting diodes](#)

*Appl. Phys. Lett.* **85**, 142 (2004); 10.1063/1.1768297

[GaN-free transparent ultraviolet light-emitting diodes](#)

*Appl. Phys. Lett.* **82**, 1 (2003); 10.1063/1.1533851

---

The advertisement features a dark blue background with white and orange text. At the top left, it reads 'NEW! Asylum Research MFP-3D Infinity™ AFM' in large white letters, followed by 'Unmatched Performance, Versatility and Support' in orange. To the right is the Oxford Instruments logo, which includes the text 'OXFORD INSTRUMENTS' and 'The Business of Science®'. Below the main text are four images: a textured surface, a circular pattern, a grid of small squares, and a photograph of the AFM instrument. Each image is accompanied by a short text description: 'Stunning high performance', 'Simpler than ever to GetStarted™', 'Comprehensive tools for nanomechanics', and 'Widest range of accessories for materials science and bioscience'.

## III-nitride ultraviolet light-emitting diodes with delta doping

K. H. Kim, J. Li, S. X. Jin, J. Y. Lin, and H. X. Jiang<sup>a)</sup>

*Department of Physics, Kansas State University, Manhattan, Kansas 66506-2601*

(Received 18 December 2002; accepted 19 May 2003)

We present the results on the fabrication and characterization of 340 nm UV light-emitting diodes (LEDs) based on InAlGaN quaternary alloys grown by metalorganic chemical vapor deposition. By employing  $\delta$  doping in the  $n$ - and  $p$ -type layers, we have demonstrated enhanced LED structural quality and emission efficiency. Combining with our interconnected microdisk LED architecture, the output power of a  $300 \times 300 \mu\text{m}^2$  bare LED chip measured from the sapphire side reached  $50 \mu\text{W}$  under a standard dc operation condition (20 mA) at 4.6 V and 1.6 mW under a pulsed driving current. © 2003 American Institute of Physics. [DOI: 10.1063/1.1593212]

Currently, there is a great need of solid-state UV emitters for many applications, ranging from the fluorescence detection of chemical and biological agents to the next generation solid-state lighting. Other applications include the use of compact UV sources ( $\lambda < 350$  nm) in medical and health research. For example, protein fluorescence is generally excited by UV light and changes in intrinsic fluorescence can be used to monitor structural changes in a protein.<sup>1</sup> Thus, the availability of chip-scale UV light sources may open new avenues for medical research. Rapid progress has been made recently in the area of III-nitride UV emitters.<sup>2-5</sup> However, the attainment of highly conductive  $p$ -type GaN and AlGaIn remains one of the biggest obstacles for the III-nitride research. Recently, we have investigated Mg- $\delta$ -doping in GaN and AlGaIn epilayers by metalorganic chemical vapor deposition (MOCVD). It was demonstrated through electrical, optical, and structural studies that Mg- $\delta$ -doping improves not only the  $p$ -type conduction, but also significantly suppresses the dislocation densities in  $p$ -type GaN and AlGaIn epilayers.<sup>6</sup> It was argued that the observed dislocation density reduction (of about one order of magnitude) is due to the growth interruption during  $\delta$  doping that partially terminates the dislocation propagation in the growth direction. Furthermore,  $\delta$  doping also reduces impurity self-compensation and enhances free carrier concentrations in  $\delta$ -doped GaN or AlGaIn.

In this work, we have incorporated Si and Mg-delta-doping into the 340 nm UV light-emitting-diode (LED) structure. The fabrication and characteristics of these UV LEDs are reported here. Figure 1 shows the schematic diagram of the UV LED structure grown by MOCVD. A Si- $\delta$ -doped  $n$ -type  $\text{Al}_x\text{Ga}_{1-x}\text{N}$  ( $x=0.2$ ) epilayer with a total thickness of  $2 \mu\text{m}$  deposited on sapphire (0001) substrate with a low temperature AlN buffer served as a template for the subsequent growth of the LED structure. The active region of the UV LED was a single quantum well consisting of  $\text{In}_{0.03}\text{Al}_{0.2}\text{Ga}_{0.77}\text{N}/\text{In}_{0.03}\text{Al}_{0.11}\text{Ga}_{0.86}\text{N}/\text{In}_{0.03}\text{Al}_{0.2}\text{Ga}_{0.77}\text{N}$  layers. The structure was capped by a 20 nm Mg-doped  $\text{Al}_{0.35}\text{Ga}_{0.65}\text{N}$  electron blocking layer and finally terminated by a  $0.15\text{-}\mu\text{m}$ -thick Mg- $\delta$ -doped GaN epilayer. The metalorganic sources used were trimethylgallium for Ga, trimethyl-

aluminum for Al, and trimethylindium for In. For Mg doping of AlGaIn, bis-cyclopentadienyl-magnesium was transported into the growth chamber with ammonia during growth. The gas sources used were blue ammonia for N,  $\text{SiH}_4$  for Si doping, and  $\text{H}_2$  as the carrier gas.  $\delta$ -junction-like doping profiles were implemented by interrupting the usual crystal-growth mode by closing the Ga and Al flows, while the Si (or Mg) impurities were introduced into the growth chamber. Postgrowth annealing was carried out at  $950^\circ\text{C}$  in nitrogen gas ambient for 8 s to activate Mg acceptors. Identical LED structures with Si- and Mg-uniformly doped  $n$ - and  $p$ -type layers were also grown for comparison studies.

By employing Si- $\delta$  doping, we found that the etch pit density in the underneath AlGaIn template can be reduced by a factor of more than 2. This is illustrated in Fig. 2, where the atomic force microscope (AFM) images are shown for the morphologies of etched surfaces after a  $0.5 \mu\text{m}$  removal for both (a) Si-uniform and (b) Si- $\delta$ -doped  $n$ -type AlGaIn underneath epilayer templates. Figure 2 clearly demonstrates a reduction of etch pit density in the Si- $\delta$ -doped  $\text{Al}_{0.2}\text{Ga}_{0.8}\text{N}$  epilayer. Although the etch pit density is not a direct measure of the dislocation density, it was shown in a series of previous work that the reduction of etch pit density implies a reduction in dislocation density.<sup>7,8</sup>

We have adapted our previously developed interconnected microdisk LED architecture for the fabrication of UV LEDs for enhancing the extraction efficiency.<sup>9</sup> Intercon-

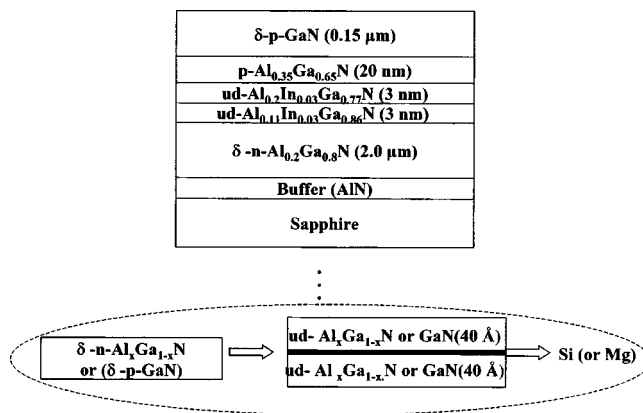


FIG. 1. Schematic diagram of a 340 nm UV LED structure incorporating Mg and Si- $\delta$  doping in  $p$ - and  $n$ -AlGaIn epilayers.

<sup>a)</sup>Electronic mail: jiang@phys.ksu.edu

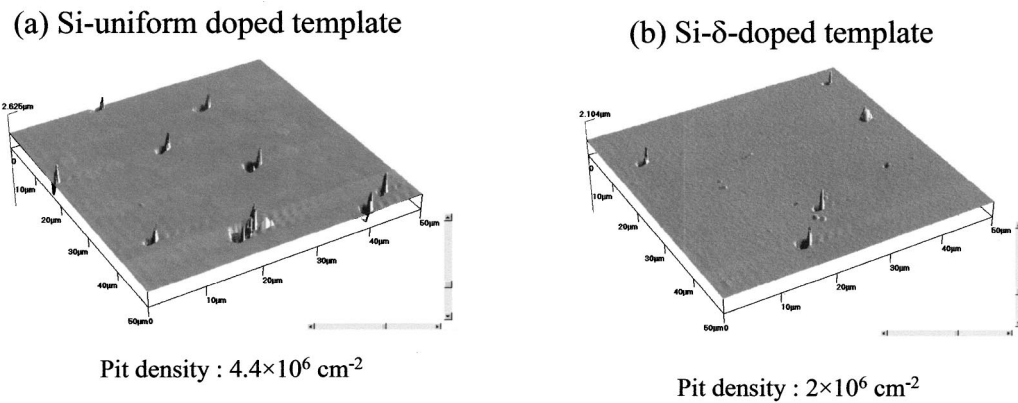


FIG. 2. AFM morphologies of etched surfaces of *n*-type AlGaN epilayer templates after a 0.5  $\mu\text{m}$  removal by ICP etching for (a) uniformly Si-doped and (b) Si- $\delta$ -doped *n*-type AlGaN epilayer. AFM images reveal that the etch pit density was significantly reduced in  $\delta$ -doped *n*-type AlGaN, implying a reduction of the dislocation density in  $\delta$ -doped AlGaN.

nected  $\mu$ -disk LEDs with individual  $\mu$ -disk diameters  $d=10 \mu\text{m}$  were fabricated from both  $\delta$ -doped and uniformly doped LED structures by photolithographic patterning and inductively coupled plasma (ICP) dry etching. Bilayers of Ni (20 nm) Au (200 nm) and Al (300 nm)/Ti (20 nm) were deposited by electron beam evaporation as *p*- and *n*-type Ohmic contacts. The contacts were thermally annealed in nitrogen ambient at 650  $^{\circ}\text{C}$  for 5 min. The detailed interconnected  $\mu$ -disk LED fabrication procedures can be found elsewhere.<sup>9,10</sup> Figure 3 shows the optical microscope images and the electroluminescence (EL) emission spectrum of representative 340 nm UV LEDs with a chip area of  $300 \times 300 \mu\text{m}^2$ . Figure 4 plots the  $I$ - $V$  and  $L$ - $I$  characteristics of 340 nm UV LEDs with  $\delta$ -doped *n*- and *p*-type layers. As expected, the interconnected microdisk LED architecture provides higher output powers at all input currents and a reduced operating voltage due to enhanced extraction efficiency and current density, as well as improved current spreading.<sup>9-11</sup>

Figure 4 shows that the optical power of  $\delta$ -doped LEDs at 340 nm measured from the sapphire substrate side on a bare chip is around 50  $\mu\text{W}$  under the standard operating condition (i.e., at an injection current of 20 mA) and reaches a maximum of about 120  $\mu\text{W}$  at a dc driving current of about 100 mA. The observed optical power saturation under dc operation is partly due to the low thermal conductivity of the

sapphire substrate that is of incapable removing the generated heat quickly.

In order to minimize the heating effect, we have measured the performances of our devices under pulsed driving currents. Figure 5 compares the optical power output-current ( $L$ - $I$ ) characteristics of interconnected  $\mu$ -disk UV LEDs (340 nm) under a pulsed operation for both  $\delta$ -doped and uniformly doped LED structures. It is interesting to note that the power output increases almost linearly with the driving current, which implies that the LED performance is not limited by the heating effect under this measurement scheme. It can be seen that the 340 nm LEDs with  $\delta$ -doped *n*- and *p*-type layers out performed that with uniformly doped layers at all input currents. The optical power at 340 nm measured from the sapphire substrate side on bare chips reached 1.6 mW at 1000 mA with a duty cycle of 1%.

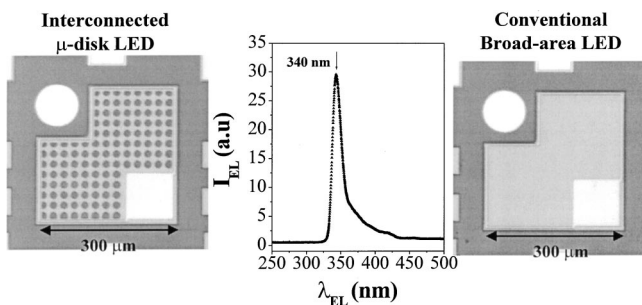


FIG. 3. Optical microscope images and the EL spectrum of our fabricated 340 nm UV LEDs showing both the interconnected  $\mu$ -disk LED and conventional LED architectures.

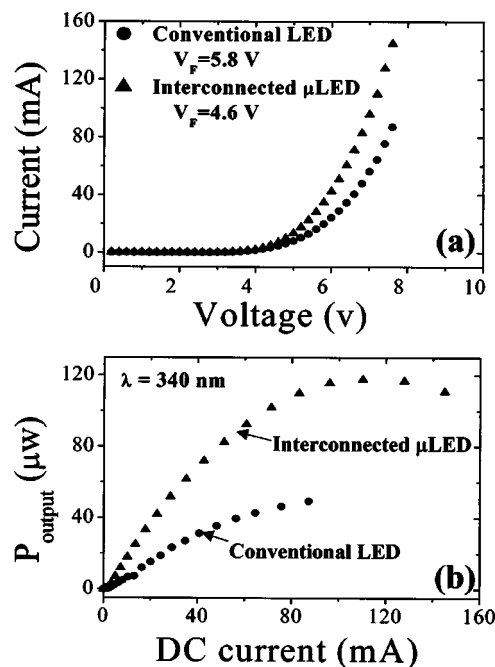


FIG. 4. (a)  $I$ - $V$  and (b)  $L$ - $I$  characteristics of our 340 nm UV LEDs showing the performances for both the interconnected  $\mu$ -disk LED and conventional LED architectures. The optical power output was measured from the sapphire substrate side on bare chips.

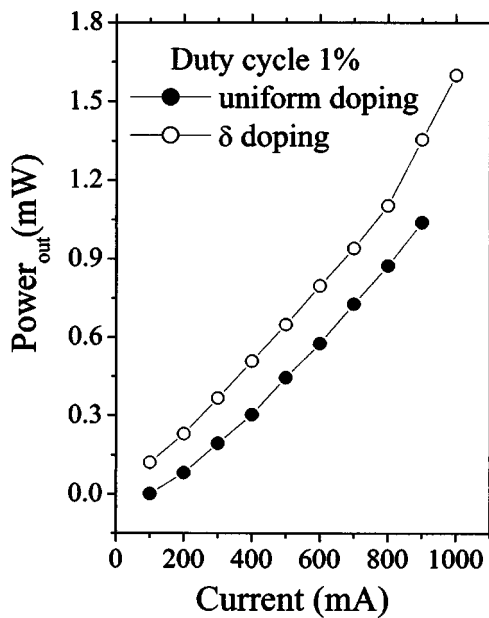


FIG. 5. Comparison of  $L$ - $I$  characteristics of interconnected  $\mu$ -disk UV (340 nm) LEDs for  $\delta$ -doped and uniform-doped structures under a pulsed driving current (pulse frequency 20 MHz, pulse width 50 ns, duty cycle 1%). The optical power output was measured from the sapphire substrate side on bare chips.

In summary, InAlGa<sub>N</sub> quaternary based 340 nm UV LED structures have been grown by MOCVD. We have achieved improved performance by employing  $\delta$  doping in the  $n$ - and  $p$ -type epilayers together with an interconnected

microdisk LED architecture. The 340 nm UV LEDs have output powers of 150  $\mu$ W at a dc driving current of 100 mA and 1.6 mW at a pulsed driving current of 1000 mA with a duty cycle of 1%.

The authors wish to acknowledge support by grants from DARPA, BMDO, ARO, NSF, DOE, and ONR.

- <sup>1</sup>J. R. Lakowicz, *Principles of Fluorescence Spectroscopy*, 2nd edition (Kluwer Academic, New York, 1999).
- <sup>2</sup>A. Chitnis, J. Sun, V. Mandavilli, R. Pachipulusu, S. Wu, M. Gaevski, V. Adivarahan, J. P. Zhang, M. Asif Khan, A. Sarua, and M. Kuball, *Appl. Phys. Lett.* **81**, 3491 (2002).
- <sup>3</sup>V. Adivarahan, A. Chitnis, J. P. Zhang, M. Shatalov, J. W. Yang, G. Simin, M. Asif Khan, R. Gaska, and M. S. Shur, *Appl. Phys. Lett.* **79**, 4240 (2001).
- <sup>4</sup>A. Yasan, R. McClintock, K. Mayes, S. R. Darvish, P. Kung, and M. Razeghi, *Appl. Phys. Lett.* **81**, 801 (2002).
- <sup>5</sup>T. Wang, Y. H. Liu, Y. B. Lee, J. P. Ao, J. Bai, and S. Sakai, *Appl. Phys. Lett.* **81**, 2508 (2002).
- <sup>6</sup>M. L. Nakarmi, K. H. Kim, J. Li, J. Y. Lin, and H. X. Jiang, *Appl. Phys. Lett.* (submitted).
- <sup>7</sup>M. Iwaya, T. Takeuchi, S. Yamaguchi, C. Wetzel, H. Amano, and I. Akasaki, *Jpn. J. Appl. Phys., Part 2* **37**, L316 (1998).
- <sup>8</sup>H. Amano, M. Iwaya, T. Kashima, M. Katsuragawa, I. Akasaki, J. Han, S. Hearne, J. A. Floro, E. Chason, and J. Figiel, *Jpn. J. Appl. Phys., Part 2* **37**, L1540 (1998).
- <sup>9</sup>S. X. Jin, J. Li, J. Z. Li, J. Y. Lin, and H. X. Jiang, *Appl. Phys. Lett.* **76**, 631 (2000).
- <sup>10</sup>S. X. Jin, J. Li, J. Y. Lin, and H. X. Jiang, *Appl. Phys. Lett.* **77**, 3236 (2000).
- <sup>11</sup>H. X. Jiang, S. X. Jin, J. Li, J. Shakya, and J. Y. Lin, *Appl. Phys. Lett.* **78**, 1303 (2001).